Advances in Aircraft and Spacecraft Science, *Vol. 7, No. 2 (2020) 169-186*
DOI: https://doi.org/10.12989/aas.2020.7.2.169

Mechanical-hygro-thermal vibrations of functionally graded porous plates with nonlocal and strain gradient effects

Raad M. Fenjan, Luay Badr Hamad and Nadhim M. Faleh*

Al-Mustansiriah University, Engineering Collage P.O. Box 46049, Bab-Muadum, Baghdad 10001, Iraq

(Received July 29, 2019, Revised October 20, 2019, Accepted October 27, 2019)

Abstract. Based upon differential quadrature method (DQM) and nonlocal strain gradient theory (NSGT), mechanical-hygro-thermal vibrational analyzes of shear deformable porous functionally graded (FG) nanoplate on visco-elastic medium has been performed. The presented formulation incorporates two scale factors for examining vibrational behaviors of nano-dimension plates more accurately. The material properties for FG plate are porosity-dependent and defined employing a modified power-law form. It is supposed that the nano-size plate is exposed to hygro-thermal and variable compressive mechanical loadings. The governing equations achieved by Hamilton's principle are solved implementing DQM. Presented results indicate the prominence of moisture/temperature variation, damping factor, material gradient index, nonlocal coefficient, strain gradient coefficient and porosities on vibrational frequencies of FG nano-size plate.

Keywords: porous plate; hygro-thermal load; nonlocal effect; four-variable plate model; differential quadrature method

1. Introduction

In a FG material, all material properties may change from one side to another side by means of a prescribed distribution. These two sides may be ceramic or metal. Mechanical characteristics of a FG material can be described based on the percentages of ceramic and metal phases. The material distribution in FG materials may be characterized via a power-law function. FG materials are not always perfect because of porosity production in them. Existence of porosities in the FG materials may significantly change their mechanical characteristics. For example, the elastic moduli of porous FG material is smaller than that of perfect FG material. Up to now, many authors focused on wave propagation, vibration and buckling analyzes of FG structures having porosities (Jabari *et al.* 2008, Chikh *et al.* 2016, Sobhy 2016, Lal *et al.* 2017, Bensaid and Keboura 2019, Zenkour and Aljadani 2018, Bekhadda *et al.* 2019). Also, there are several investigations concerning with the analysis of FG structures in thermal environments (Bouderba *et al.* 2016, El-Hassar *et al.* 2016).

Recently, this kind of materials have found their applications in nano-scale structures. Vibration behavior of a nano-scale plate is not the same as a macro-scale plate (Lee *et al.* 2006, Zalesak *et al.* 2016). This is because small-size effects are not present at macro scale. So, mathematical modeling of a nanoplate can be done with the use of nonlocal elasticity (Eringen 1983)

*Corresponding author, Professor, E-mail: dr.nadhim@uomustansiriyah.edu.iq, drnadhim@gmail.com

http://www.techno-press.org/?journal=aas&subpage=7 ISSN: 2287-528X (Print), 2287-5271 (Online)

incorporating only one scale parameter (Berrabah *et al.* 2013, Zenkour and Abouelregal 2014, Aissani *et al.* 2015, Besseghier *et al.* 2015, 2017, Elmerabet *et al.* 2017, Bouadi *et al.* 2018, Yazid *et al.* 2018). Due to the ignorance of strain gradient effect in nonlocal elasticity theory, a more general theory will be required (Natarajan *et al.* 2012, Daneshmehr and Rajabpoor 2014, Belkorissat *et al.* 2015, Ebrahimi and Barati 2016a, Sobhy 2015, Sobhy and Radwan 2017, Larbi Chaht *et al.* 2015, Belmahi *et al.* 2019, Al-assadi *et al.* 2019). Strain gradients at nano-scale are observed by many researchers (Lam *et al.* 2003, Lim *et al.* 2015, Mirsalehi *et al.* 2017). Thus, nonlocal-strain gradient theory was introduced as a general theory which contains an additional strain gradient parameter together with nonlocal parameter (Li *et al.* 2015& 2016, Li and Hu 2015&2016&2017, Ebrahimi and Barati 2017, Barati and Zenkour 2017, Fenjan *et al.* 2019). The scale parameters used in nonlocal strain gradient theory can be obtained by fitting obtained theoretical results with available experimental data and even molecular dynamic (MD) simulations.

This paper uses a higher order shear deformation plate formulation having four variables without using of shear correction factor. Based upon differential quadrature (DQ) approach and nonlocal strain gradient (NSGT) formulation, mechanical-hygro-thermal vibrational analysis of shear deformable porous functionally graded (FG) nanoplate on visco-elastic medium has been performed. The presented formulation incorporates two scale factors for examining vibrational behaviors of nano-dimension plates more accurately. The material properties for FG plate are porosity-dependent and defined employing a modified power-law form. It is supposed that the nano-sized plate is exposed to hygro-thermal and variable compressive mechanical loadings. The governing equations achieved by Hamilton's principle are solved implementing DQM. Presented results indicate the prominence of moisture/temperature variation, damping factor, material gradient index, nonlocal coefficient, strain gradient coefficient and porosities on vibrational frequencies of FG nano-size plate.

2. Nanoplate modeling based on NSGT

In the well-known nonlocal strain gradient theory (Lim *et al.* 2015), strain gradient impacts are taken into accounting together with nonlocal stress influences defined in below relation:

$$\sigma_{ij} = \sigma_{ij}^{(0)} - \nabla \sigma_{ij}^{(1)} \tag{1}$$

in such a way that stress $\sigma ij^{(0)}$ is corresponding to strain components ε_{kl} and a higher order stress is related to strain gradient components $\nabla\varepsilon_{kl}$ which are (Lim *et al.* 2015):

$$\sigma_{ij}^{(0)} = \int_V C_{ijkl}\alpha_0(x,x',e_0a)\varepsilon'_{kl}(x')dx' \tag{2a}$$

$$\sigma_{ij}^{(1)} = l^2 \int_V C_{ijkl}\alpha_1(x,x',e_1a)\nabla\varepsilon'_{kl}(x')dx' \tag{2b}$$

in which C_{ijkl} express the elastic properties; Also, e_0a and e_1a are corresponding to nonlocality impacts and l is related to strains gradients. Whenever two nonlocality functions $\alpha 0(x, x', e_0a)$ and

$\alpha 1(x, x', e_1 a)$ verify Eringen's announced conditions, NSGT constitutive relation may be written as follows:

$$[1-(e_1a)^2\nabla^2][1-(e_0a)^2\nabla^2]\sigma_{ij} = C_{ijkl}[1-(e_1a)^2\nabla^2]\varepsilon_{kl} - C_{ijkl}\, l^2[1-(e_0a)^2\nabla^2]\nabla^2\varepsilon_{kl} \quad (3)$$

so that ∇^2 defines the operator for Laplacian; by selecting $e_1=e_0=e$, above relationship decreases to:

$$[1-(ea)^2\nabla^2]\sigma_{ij} = C_{ijkl}[1-l^2\nabla^2]\varepsilon_{kl} \quad (4)$$

Taking into account the temperature/humidity impact Eq. (4) might be rewritten as (Ebrahimi and Barati 2017):

$$[1-(ea)^2\nabla^2]\sigma_{ij} = C_{ijkl}[1-l^2\nabla^2](\varepsilon_{kl} - \gamma_{ij}T - \beta_{ij}C) \quad (5)$$

so that γ_{ij} and β_{ij} respectively define the temperature and humidity expansion properties.

3. Modeling FG plates having porosity

For the nanoplate shown in Fig.1, the material distribution in FG materials may be characterized via a power-law function. FG materials are not always perfect because of porosity production in them. Existence of porosities in the FG materials may significantly change their mechanical characteristics. Depending on the type of porosity distribution, the elastic moduli E, density ρ, temperature expansion property γ and humidity expansion property β for porous FG material can be expressed in the following power-law form having material gradient index p as (Barati and Zenkour 2017):

$$E(z) = (E_c - E_m)\left(\frac{z}{h}+\frac{1}{2}\right)^p + E_m - \frac{\alpha}{2}(E_c + E_m) \quad (6a)$$

$$\rho(z) = (\rho_c - \rho_m)\left(\frac{z}{h}+\frac{1}{2}\right)^p + \rho_m - \frac{\alpha}{2}(\rho_c + \rho_m) \quad (6b)$$

$$\gamma(z) = (\gamma_c - \gamma_m)\left(\frac{z}{h}+\frac{1}{2}\right)^p + \gamma_m - \frac{\alpha}{2}(\gamma_c + \gamma_m) \quad (6c)$$

$$\beta(z) = (\beta_c - \beta_m)\left(\frac{z}{h}+\frac{1}{2}\right)^p + \beta_m - \frac{\alpha}{2}(\beta_c + \beta_m) \quad (6d)$$

where m and c corresponds to the metallic and ceramic sides, respectively; α defines the porosity volume fraction.

By defining exact location of neutral surface, the displacement components based on axial u, lateral v, bending w_b and shear w_s displacements may be introduced as (Besseghier *et al.* 2017, Fenjan *et al.* 2019):

$$u_x(x,y,z,t) = u(x,y,t) - (z - r^*)\frac{\partial w_b}{\partial x} - [\Upsilon(z) - r^{**}]\frac{\partial w_s}{\partial x} \tag{7a}$$

$$u_y(x,y,z,t) = v(x,y,t) - (z - r^*)\frac{\partial w_b}{\partial y} - [\Upsilon(z) - r^{**}]\frac{\partial w_s}{\partial y} \tag{7b}$$

$$u_z(x,y,z,t) = w(x,y,t) = w_b + w_s \tag{7c}$$

so that

$$r^* = \int_{-h/2}^{h/2} E(z)\, z dz \Big/ \int_{-h/2}^{h/2} E(z)\, dz\,, \qquad r^{**} = \int_{-h/2}^{h/2} E(z)\Upsilon(z) dz \Big/ \int_{-h/2}^{h/2} E(z)\, dz \tag{8}$$

Here, third order shear function is employed as:

$$\Upsilon(z) = -\frac{z}{4} + \frac{5z^3}{3h^2} \tag{9}$$

Finally, the strains based on the four-unknown plate model have been obtained as:

$$\begin{aligned}
\varepsilon_x &= \frac{\partial u}{\partial x} - (z - r^*)\frac{\partial^2 w_b}{\partial x^2} - [\Upsilon(z) - r^{**}]\frac{\partial^2 w_s}{\partial x^2} \\
\varepsilon_y &= \frac{\partial v}{\partial y} - (z - r^*)\frac{\partial^2 w_b}{\partial y^2} - [\Upsilon(z) - r^{**}]\frac{\partial^2 w_s}{\partial y^2} \\
\gamma_{xy} &= \frac{\partial u}{\partial y} + \frac{\partial v}{\partial x} - 2(z - r^*)\frac{\partial^2 w_b}{\partial x \partial y} - 2[\Upsilon(z) - r^{**}]\frac{\partial^2 w_s}{\partial x \partial y} \\
\gamma_{yz} &= g(z)\frac{\partial w_s}{\partial y}, \quad \gamma_{xz} = g(z)\frac{\partial w_s}{\partial x}
\end{aligned} \tag{10}$$

Next, one might express the Hamilton's rule as follows based on strain energy (U) and kinetic energy (T):

$$\int_0^t \delta(U - T + V)\, dt = 0 \tag{11}$$

and V is the work of non-conservative loads. Based on above relation we have:

$$\begin{aligned}
\delta U = \int_V (&\sigma_{xx}\delta\varepsilon_{xx} + \sigma_{xx}^{(1)}\delta\nabla\varepsilon_{xx} + \sigma_{yy}\delta\varepsilon_{yy} + \sigma_{yy}^{(1)}\delta\nabla\varepsilon_{yy} + \sigma_{xy}\delta\gamma_{xy} + \sigma_{xy}^{(1)}\delta\nabla\gamma_{xy} \\
&+ \sigma_{yz}\delta\gamma_{yz} + \sigma_{yz}^{(1)}\delta\nabla\gamma_{yz} + \sigma_{xz}\delta\gamma_{xz} + \sigma_{xz}^{(1)}\delta\nabla\gamma_{xz})\, dV
\end{aligned} \tag{12}$$

Note that for obtaining Eq.(12), the thickness effects discussed by Tang *et al.* (2019) have been neglected by the authors. Placing Eqs. (8) and (10) in Eq.(12) leads to:

$$\delta U=\int_0^a\int_0^b[N_{xx}[\frac{\partial\delta u}{\partial x}+\frac{\partial w}{\partial x}\frac{\partial\delta w}{\partial x}]-M_{xx}^b\frac{\partial^2\delta w_b}{\partial x^2}-M_{xx}^s\frac{\partial^2\delta w_s}{\partial x^2}+N_{yy}[\frac{\partial\delta v}{\partial y}+\frac{\partial w}{\partial y}\frac{\partial\delta w}{\partial y}]$$
$$-M_{yy}^b\frac{\partial^2\delta w_b}{\partial y^2}-M_{yy}^s\frac{\partial^2\delta w_s}{\partial y^2}+N_{xy}(\frac{\partial\delta u}{\partial y}+\frac{\partial\delta v}{\partial x}+\frac{\partial w}{\partial x}\frac{\partial\delta w}{\partial y}+\frac{\partial w}{\partial y}\frac{\partial\delta w}{\partial x})-2M_{xy}^b\frac{\partial^2\delta w_b}{\partial x\partial y} \quad (13)$$
$$-2M_{xy}^s\frac{\partial^2\delta w_s}{\partial x\partial y}+Q_{yz}\frac{\partial\delta w_s}{\partial y}+Q_{xz}\frac{\partial\delta w_s}{\partial x}]dydx$$

in which:

$$\begin{aligned}
N_{xx}&=\int_{-h/2}^{h/2}(\sigma_{xx}^0-\nabla\sigma_{xx}^{(1)})dz=N_{xx}^{(0)}-\nabla N_{xx}^{(1)}\\
N_{xy}&=\int_{-h/2}^{h/2}(\sigma_{xy}^0-\nabla\sigma_{xy}^{(1)})dz=N_{xy}^{(0)}-\nabla N_{xy}^{(1)}\\
N_{yy}&=\int_{-h/2}^{h/2}(\sigma_{yy}^0-\nabla\sigma_{yy}^{(1)})dz=N_{yy}^{(0)}-\nabla N_{yy}^{(1)}\\
M_{xx}^b&=\int_{-h/2}^{h/2}z(\sigma_{xx}^0-\nabla\sigma_{xx}^{(1)})dz=M_{xx}^{b(0)}-\nabla M_{xx}^{b(1)}\\
M_{xx}^s&=\int_{-h/2}^{h/2}f(\sigma_{xx}^0-\nabla\sigma_{xx}^{(1)})dz=M_{xx}^{s(0)}-\nabla M_{xx}^{s(1)}\\
M_{yy}^b&=\int_{-h/2}^{h/2}z(\sigma_{yy}^0-\nabla\sigma_{yy}^{(1)})dz=M_{yy}^{b(0)}-\nabla M_{yy}^{b(1)}\\
M_{yy}^s&=\int_{-h/2}^{h/2}f(\sigma_{yy}^0-\nabla\sigma_{yy}^{(1)})dz=M_{yy}^{s(0)}-\nabla M_{yy}^{s(1)}\\
M_{xy}^b&=\int_{-h/2}^{h/2}z(\sigma_{xy}^0-\nabla\sigma_{xy}^{(1)})dz=M_{xy}^{b(0)}-\nabla M_{xy}^{b(1)}\\
M_{xy}^s&=\int_{-h/2}^{h/2}f(\sigma_{xy}^0-\nabla\sigma_{xy}^{(1)})dz=M_{xy}^{s(0)}-\nabla M_{xy}^{s(1)}\\
Q_{xz}&=\int_{-h/2}^{h/2}g(\sigma_{xz}^0-\nabla\sigma_{xz}^{(1)})dz=Q_{xz}^{(0)}-\nabla Q_{xz}^{(1)}\\
Q_{yz}&=\int_{-h/2}^{h/2}g(\sigma_{yz}^0-\nabla\sigma_{yz}^{(1)})dz=Q_{yz}^{(0)}-\nabla Q_{yz}^{(1)}
\end{aligned} \quad (14a)$$

where

$$\begin{aligned}
N_{ij}^{(0)}&=\int_{-h/2}^{h/2}(\sigma_{ij}^{(0)})dz,\quad N_{ij}^{(1)}=\int_{-h/2}^{h/2}(\sigma_{ij}^{(1)})dz\\
M_{ij}^{b(0)}&=\int_{-h/2}^{h/2}z(\sigma_{ij}^{b(0)})dz,\quad M_{ij}^{b(1)}=\int_{-h/2}^{h/2}z(\sigma_{ij}^{b(1)})dz\\
M_{ij}^{s(0)}&=\int_{-h/2}^{h/2}f(\sigma_{ij}^{s(0)})dz,\quad M_{ij}^{s(1)}=\int_{-h/2}^{h/2}f(\sigma_{ij}^{s(1)})dz\\
Q_{xz}^{(0)}&=\int_{-h/2}^{h/2}g(\sigma_{xz}^{i(0)})dz,\quad Q_{xz}^{(1)}=\int_{-h/2}^{h/2}g(\sigma_{xz}^{i(1)})dz\\
Q_{yz}^{(0)}&=\int_{-h/2}^{h/2}g(\sigma_{yz}^{i(0)})dz,\quad Q_{yz}^{(1)}=\int_{-h/2}^{h/2}g(\sigma_{yz}^{i(1)})dz
\end{aligned} \quad (14b)$$

for which (*ij=xx, xy, yy*). The variation for the work of non-conservative force is expressed by:

$$\begin{aligned}\delta V=\int_0^a\int_0^b(N_x^0\frac{\partial(w_b+w_s)}{\partial x}\frac{\partial\delta(w_b+w_s)}{\partial x}+N_y^0\frac{\partial(w_b+w_s)}{\partial y}\frac{\partial\delta(w_b+w_s)}{\partial y}\\+2\delta N_{xy}^0\frac{\partial(w_b+w_s)}{\partial x}\frac{\partial(w_b+w_s)}{\partial y}-k_w(w_b+w_s)\delta(w_b+w_s)-c_d\delta\frac{\partial(w_b+w_s)}{\partial t}\\+k_p(\frac{\partial(w_b+w_s)}{\partial x}\frac{\partial\delta(w_b+w_s)}{\partial x}+\frac{\partial(w_b+w_s)}{\partial y}\frac{\partial\delta(w_b+w_s)}{\partial y}))dydx\end{aligned}\tag{15a}$$

where N_x^0, N_y^0, N_{xy}^0 denote membrane forces; k_w, k_p and c_d are viscoelastic substrate constants. Herein, the nano-dimension plate has been exposed to the below in-plane loading while shearing load has been neglected N^0_{xy}=0:

$$\begin{aligned}N_x^0=N^T+N^H+N_x^M,\quad N_y^0=N^T+N^H+N_y^M\\N_x^0=N(1-\xi\frac{y}{b}),\quad N_y^0=\eta N(1-\xi\frac{x}{a})\end{aligned}\tag{15b}$$

where hygro-thermal resultants may be defined as:

$$\begin{aligned}N^T=\int_{-h/2}^{h/2}\frac{E(z)}{1-v}\gamma(z)(T-T_0)\,dz\\N^H=\int_{-h/2}^{h/2}\frac{E(z)}{1-v}\beta(z)(C-C_0)\,dz\end{aligned}\tag{15c}$$

so that $C=\Delta C+C_0$ and $T=\Delta T+T_0$ define humidity and temperature variations; C_0 and T_0 express prescribed humidity and temperature. Then, applied compressive loading may be defined as:

$$N_x^M=N(1-\xi\frac{y}{b}),\quad N_y^M=N(1-\xi\frac{x}{a})\tag{15d}$$

Also, the kinetic energy variation is obtained as:

$$\begin{aligned}\delta K=\int_0^a\int_0^b[I_0(\frac{\partial u}{\partial t}\frac{\partial\delta u}{\partial t}+\frac{\partial v}{\partial t}\frac{\partial\delta v}{\partial t}+\frac{\partial(w_b+w_s)}{\partial t}\frac{\partial\delta(w_b+w_s)}{\partial t})-I_1(\frac{\partial u}{\partial t}\frac{\partial\delta w_b}{\partial x\partial t}+\frac{\partial w_b}{\partial x\partial t}\frac{\partial\delta u}{\partial t}+\frac{\partial v}{\partial t}\frac{\partial\delta w_b}{\partial y\partial t}\\+\frac{\partial w_b}{\partial y\partial t}\frac{\partial\delta v}{\partial t})-I_3(+\frac{\partial w_s}{\partial y\partial t}\frac{\partial\delta v}{\partial t}+\frac{\partial w_s}{\partial x\partial t}\frac{\partial\delta u}{\partial t}+\frac{\partial u}{\partial t}\frac{\partial\delta w_s}{\partial x\partial t}+\frac{\partial v}{\partial t}\frac{\partial\delta w_s}{\partial y\partial t})+I_2(+\frac{\partial w_b}{\partial y\partial t}\frac{\partial\delta w_b}{\partial y\partial t}+\frac{\partial w_b}{\partial x\partial t}\frac{\partial\delta w_b}{\partial x\partial t})\\+I_5(+\frac{\partial w_s}{\partial y\partial t}\frac{\partial\delta w_s}{\partial y\partial t}+\frac{\partial w_s}{\partial x\partial t}\frac{\partial\delta w_s}{\partial x\partial t})+I_4(\frac{\partial w_b}{\partial x\partial t}\frac{\partial\delta w_s}{\partial x\partial t}+\frac{\partial w_s}{\partial y\partial t}\frac{\partial\delta w_b}{\partial y\partial t}+\frac{\partial w_s}{\partial x\partial t}\frac{\partial\delta w_b}{\partial x\partial t}+\frac{\partial w_b}{\partial y\partial t}\frac{\partial\delta w_s}{\partial y\partial t})]dydx\end{aligned}\tag{16}$$

so that

$$(I_0,I_1,I_2,I_3,I_4,I_5)=\int_{-h/2}^{h/2}(1,z-r^*,(z-r^*)^2,\Upsilon-r^{**},(z-r^*)(\Upsilon-r^{**}),(\Upsilon-r^{**})^2)\rho(z)dz\tag{17}$$

Substituting Eqs.(13)-(16) into Eq.(11) then collecting the coefficients for field variables results in four equations of motion:

$$\frac{\partial N_x}{\partial x}+\frac{\partial N_{xy}}{\partial y}=I_0\frac{\partial^2 u}{\partial t^2}-I_1\frac{\partial^3 w_b}{\partial x\partial t^2}-I_3\frac{\partial^3 w_s}{\partial x\partial t^2} \tag{18}$$

$$\frac{\partial N_{xy}}{\partial x}+\frac{\partial N_y}{\partial y}=I_0\frac{\partial^2 v}{\partial t^2}-I_1\frac{\partial^3 w_b}{\partial y\partial t^2}-I_3\frac{\partial^3 w_s}{\partial y\partial t^2} \tag{19}$$

$$\begin{aligned}&\frac{\partial^2 M_x^b}{\partial x^2}+2\frac{\partial^2 M_{xy}^b}{\partial x\partial y}+\frac{\partial^2 M_y^b}{\partial y^2}-(N^T+N^H-k_p)[\frac{\partial^2(w_b+w_s)}{\partial x^2}+\frac{\partial^2(w_b+w_s)}{\partial y^2}]\\&-N_x^M(y)\frac{\partial^2(w_b+w_s)}{\partial x^2}-N_y^M(x)\frac{\partial^2(w_b+w_s)}{\partial y^2}-k_w(w_b+w_s)-c_d\frac{\partial(w_b+w_s)}{\partial t}=\\&I_0\frac{\partial^2(w_b+w_s)}{\partial t^2}+I_1(\frac{\partial^3 u}{\partial x\partial t^2}+\frac{\partial^3 v}{\partial y\partial t^2})-I_2(\frac{\partial^2}{\partial x^2}+\frac{\partial^2}{\partial y^2})(\frac{\partial^2 w_b}{\partial t^2})-I_4(\frac{\partial^2}{\partial x^2}+\frac{\partial^2}{\partial y^2})(\frac{\partial^2 w_s}{\partial t^2})\end{aligned} \tag{20}$$

$$\begin{aligned}&\frac{\partial^2 M_x^s}{\partial x^2}+2\frac{\partial^2 M_{xy}^s}{\partial x\partial y}+\frac{\partial^2 M_y^s}{\partial y^2}+\frac{\partial Q_{xz}}{\partial x}+\frac{\partial Q_{yz}}{\partial y}-(N^T+N^H-k_p)[\frac{\partial^2(w_b+w_s)}{\partial x^2}+\frac{\partial^2(w_b+w_s)}{\partial y^2}]\\&-N_x^M(y)\frac{\partial^2(w_b+w_s)}{\partial x^2}-N_y^M(x)\frac{\partial^2(w_b+w_s)}{\partial y^2}-k_w(w_b+w_s)-c_d\frac{\partial(w_b+w_s)}{\partial t}=I_0\frac{\partial^2(w_b+w_s)}{\partial t^2}\\&+I_3(\frac{\partial^3 u}{\partial x\partial t^2}+\frac{\partial^3 v}{\partial y\partial t^2})-I_4(\frac{\partial^2}{\partial x^2}+\frac{\partial^2}{\partial y^2})(\frac{\partial^2 w_b}{\partial t^2})-I_5(\frac{\partial^2}{\partial x^2}+\frac{\partial^2}{\partial y^2})(\frac{\partial^2 w_s}{\partial t^2})\end{aligned} \tag{21}$$

Next, all edge conditions for $x = 0$, a and $y = 0$, b may be expressed by:

$$\begin{aligned}&\text{Specify } un_x+vn_y \text{ or } N_x n_x^2+2n_x n_y N_{xy}+N_y n_y^2=0\\&\text{Specify } -un_y+vn_x \text{ or } (N_y-N_x)n_x n_y+N_{xy}(n_x^2-n_y^2)=0\\&\text{Specify } w_b \text{ or } \left(\frac{\partial M_{xx}^b}{\partial x}+\frac{\partial M_{xy}^b}{\partial y}-I_1\frac{\partial^2 u}{\partial t^2}+I_2\frac{\partial^3 w_b}{\partial x\partial t^2}+I_4\frac{\partial^3 w_s}{\partial x\partial t^2}\right)n_x\\&\qquad+\left(\frac{\partial M_{yy}^b}{\partial y}+\frac{\partial M_{xy}^b}{\partial x}-I_1\frac{\partial^2 v}{\partial t^2}+I_2\frac{\partial^3 w_b}{\partial y\partial t^2}+I_4\frac{\partial^3 w_s}{\partial y\partial t^2}\right)n_y=0\\&\text{Specify } w_s \text{ or } \left(\frac{\partial M_{xx}^s}{\partial x}+\frac{\partial M_{xy}^s}{\partial y}+Q_{xz}-I_3\frac{\partial^2 u}{\partial t^2}+I_4\frac{\partial^3 w_b}{\partial x\partial t^2}+I_5\frac{\partial^3 w_s}{\partial x\partial t^2}\right)n_x\\&\qquad+\left(\frac{\partial M_{yy}^s}{\partial y}+\frac{\partial M_{xy}^s}{\partial x}+Q_{yz}-I_3\frac{\partial^2 v}{\partial t^2}+I_4\frac{\partial^3 w_b}{\partial y\partial t^2}+I_5\frac{\partial^3 w_s}{\partial y\partial t^2}\right)n_y=0\\&\text{Specify } \frac{\partial w_b}{\partial n} \text{ or } M_{xx}^b n_x^2+n_x n_y M_{xy}^b+M_{yy}^b n_y^2=0\end{aligned} \tag{22}$$

Note that $\frac{\partial()}{\partial n}=n_x\frac{\partial()}{\partial x}+n_y\frac{\partial()}{\partial y}$; n_x and n_y respectively define axial and lateral normal vectors at edges, and non-classic edge condition may be written as:

$$\begin{aligned} &\text{Specify } \frac{\partial^2 w_b}{\partial x^2} \text{ or } M_{xx}^{b(1)} = 0 \\ &\text{Specify } \frac{\partial^2 w_b}{\partial y^2} \text{ or } M_{yy}^{b(1)} = 0 \\ &\text{Specify } \frac{\partial^2 w_s}{\partial x^2} \text{ or } M_{xx}^{s(1)} = 0 \\ &\text{Specify } \frac{\partial^2 w_s}{\partial y^2} \text{ or } M_{yy}^{s(1)} = 0 \end{aligned} \tag{23}$$

Finally, the nonlocal strain gradient constitutive relations based on refined FG plate model can be expressed by:

$$(1-\mu\nabla^2)\begin{Bmatrix}\sigma_x\\ \sigma_y\\ \sigma_{xy}\\ \sigma_{yz}\\ \sigma_{xz}\end{Bmatrix} = \frac{E(z)}{1-v^2}(1-\lambda\nabla^2)\begin{pmatrix}1 & v & 0 & 0 & 0\\ v & 1 & 0 & 0 & 0\\ 0 & 0 & (1-v)/2 & 0 & 0\\ 0 & 0 & 0 & (1-v)/2 & 0\\ 0 & 0 & 0 & 0 & (1-v)/2\end{pmatrix}\begin{Bmatrix}\varepsilon_x-\gamma\Delta T-\beta\Delta C\\ \varepsilon_y-\gamma\Delta T-\beta\Delta C\\ \gamma_{xy}\\ \gamma_{yz}\\ \gamma_{xz}\end{Bmatrix} \tag{24}$$

After integrating Eq. (24) in thickness direction, we get to the following relationships:

$$(1-\mu\nabla^2)\begin{Bmatrix}N_x\\ N_y\\ N_{xy}\end{Bmatrix} = A(1-\lambda\nabla^2)\begin{pmatrix}1 & v & 0\\ v & 1 & 0\\ 0 & 0 & (1-v)/2\end{pmatrix}\begin{Bmatrix}\frac{\partial u}{\partial x}\\ \frac{\partial v}{\partial y}\\ \frac{\partial u}{\partial y}+\frac{\partial v}{\partial x}\end{Bmatrix} \tag{25}$$

$$(1-\mu\nabla^2)\begin{Bmatrix}M_x^b\\ M_y^b\\ M_{xy}^b\end{Bmatrix} = D(1-\lambda\nabla^2)\begin{pmatrix}1 & v & 0\\ v & 1 & 0\\ 0 & 0 & (1-v)/2\end{pmatrix}\begin{Bmatrix}-\frac{\partial^2 w_b}{\partial x^2}\\ -\frac{\partial^2 w_b}{\partial y^2}\\ -2\frac{\partial^2 w_b}{\partial x\partial y}\end{Bmatrix} + E(1-\lambda\nabla^2)\begin{pmatrix}1 & v & 0\\ v & 1 & 0\\ 0 & 0 & (1-v)/2\end{pmatrix}\begin{Bmatrix}-\frac{\partial^2 w_s}{\partial x^2}\\ -\frac{\partial^2 w_s}{\partial y^2}\\ -2\frac{\partial^2 w_s}{\partial x\partial y}\end{Bmatrix} \tag{26}$$

$$(1-\mu\nabla^2)\begin{Bmatrix}M_x^s\\ M_y^s\\ M_{xy}^s\end{Bmatrix} = E(1-\lambda\nabla^2)\begin{pmatrix}1 & v & 0\\ v & 1 & 0\\ 0 & 0 & (1-v)/2\end{pmatrix}\begin{Bmatrix}-\frac{\partial^2 w_b}{\partial x^2}\\ -\frac{\partial^2 w_b}{\partial y^2}\\ -2\frac{\partial^2 w_b}{\partial x\partial y}\end{Bmatrix} + F(1-\lambda\nabla^2)\begin{pmatrix}1 & v & 0\\ v & 1 & 0\\ 0 & 0 & (1-v)/2\end{pmatrix}\begin{Bmatrix}-\frac{\partial^2 w_s}{\partial x^2}\\ -\frac{\partial^2 w_s}{\partial y^2}\\ -2\frac{\partial^2 w_s}{\partial x\partial y}\end{Bmatrix} \tag{27}$$

$$(1-\mu\nabla^2)\begin{Bmatrix} Q_x \\ Q_y \end{Bmatrix} = A_{44}(1-\lambda\nabla^2)\begin{pmatrix} 1 & 0 \\ 0 & 1 \end{pmatrix}\begin{Bmatrix} \frac{\partial w_s}{\partial x} \\ \frac{\partial w_s}{\partial y} \end{Bmatrix} \tag{28}$$

in which:

$$\begin{aligned} &A=\int_{-h/2}^{h/2}\frac{E(z)}{1-v^2}dz,\ \ D=\int_{-h/2}^{h/2}\frac{E(z)(z-r^*)^2}{1-v^2}dz,\ \ E=\int_{-h/2}^{h/2}\frac{E(z)(z-r^*)(\Upsilon-r^{**})}{1-v^2}dz \\ &F=\int_{-h/2}^{h/2}\frac{E(z)(\Upsilon-r^{**})^2}{1-v^2}dz,\quad A_{44}=\int_{-h/2}^{h/2}\frac{E(z)}{2(1+v)}g^2dz \end{aligned} \tag{29}$$

Three equations of motion based on neutral surface location will be achieved by placing Eqs. (25)-(28) in Eqs. (18)-(21) by:

$$A(1-\lambda\nabla^2)(\frac{\partial^2 u}{\partial x^2}+\frac{1-v}{2}\frac{\partial^2 u}{\partial y^2}+\frac{1+v}{2}\frac{\partial^2 v}{\partial x\partial y})+(1-\mu\nabla^2)(-I_0\frac{\partial^2 u}{\partial t^2}+I_1\frac{\partial^3 w_b}{\partial x\partial t^2}+I_3\frac{\partial^3 w_s}{\partial x\partial t^2})=0 \tag{30}$$

$$A(1-\lambda\nabla^2)(\frac{\partial^2 v}{\partial y^2}+\frac{1-v}{2}\frac{\partial^2 v}{\partial x^2}+\frac{1+v}{2}\frac{\partial^2 u}{\partial x\partial y})+(1-\mu\nabla^2)(-I_0\frac{\partial^2 v}{\partial t^2}+I_1\frac{\partial^3 w_b}{\partial y\partial t^2}+I_3\frac{\partial^3 w_s}{\partial y\partial t^2})=0 \tag{31}$$

$$\begin{aligned} &-D(1-\lambda\nabla^2)(\frac{\partial^4 w_b}{\partial x^4}+2\frac{\partial^4 w_b}{\partial x^2\partial y^2}+\frac{\partial^4 w_b}{\partial y^4})-E(1-\lambda\nabla^2)(\frac{\partial^4 w_s}{\partial x^4}+2\frac{\partial^4 w_s}{\partial x^2\partial y^2}+\frac{\partial^4 w_s}{\partial y^4}) \\ &+(1-\mu\nabla^2)(-I_0\frac{\partial^2(w_b+w_s)}{\partial t^2}-I_1(\frac{\partial^3 u}{\partial x\partial t^2}+\frac{\partial^3 v}{\partial y\partial t^2})+I_2\nabla^2(\frac{\partial^2 w_b}{\partial t^2}) \\ &+I_4\nabla^2(\frac{\partial^2 w_s}{\partial t^2})-(N^T+N^H)[\frac{\partial^2(w_b+w_s)}{\partial x^2}+\frac{\partial^2(w_b+w_s)}{\partial y^2}]-N_x^M(y)\frac{\partial^2(w_b+w_s)}{\partial x^2} \\ &-N_y^M(x)\frac{\partial^2(w_b+w_s)}{\partial y^2}-(k_w+\frac{\partial}{\partial t}c_d)(w_b+w_s)+k_P[\frac{\partial^2(w_b+w_s)}{\partial x^2}+\frac{\partial^2(w_b+w_s)}{\partial y^2}])=0 \end{aligned} \tag{32}$$

$$\begin{aligned} &-E(1-\lambda\nabla^2)(\frac{\partial^4 w_b}{\partial x^4}+2\frac{\partial^4 w_b}{\partial x^2\partial y^2}+\frac{\partial^4 w_b}{\partial y^4})-F(1-\lambda\nabla^2)(\frac{\partial^4 w_s}{\partial x^4}+2\frac{\partial^4 w_s}{\partial x^2\partial y^2}+\frac{\partial^4 w_s}{\partial y^4}) \\ &+A_{44}(1-\lambda\nabla^2)(\frac{\partial^2 w_s}{\partial x^2}+\frac{\partial^2 w_s}{\partial y^2})+(1-\mu\nabla^2)(-I_0\frac{\partial^2(w_b+w_s)}{\partial t^2}-I_3(\frac{\partial^3 u}{\partial x\partial t^2}+\frac{\partial^3 v}{\partial y\partial t^2}) \\ &+I_4\nabla^2(\frac{\partial^2 w_b}{\partial t^2})+I_5\nabla^2(\frac{\partial^2 w_s}{\partial t^2})-(N^T+N^H)[\frac{\partial^2(w_b+w_s)}{\partial x^2}+\frac{\partial^2(w_b+w_s)}{\partial y^2}] \\ &-N_x^M(y)\frac{\partial^2(w_b+w_s)}{\partial x^2}-N_y^M(x)\frac{\partial^2(w_b+w_s)}{\partial y^2}-(k_w+\frac{\partial}{\partial t}c_d)(w_b+w_s) \\ &+k_p[\frac{\partial^2(w_b+w_s)}{\partial x^2}+\frac{\partial^2(w_b+w_s)}{\partial y^2}])=0 \end{aligned} \tag{33}$$

4. Solution by differential quadrature method (DQM)

In the present chapter, differential quadrature method (DQM) has been utilized for solving the governing equations for NSGT porous FG nanoplate. According to DQM, at an assumed grid point (x_i, y_j) the derivatives for function F are supposed as weighted linear summation of all functional values within the computation domains as:

$$\frac{d^n F}{dx^n}\bigg|_{x=x_i} = \sum_{j=1}^{N} c_{ij}^{(n)} F(x_j) \tag{34}$$

where

$$C_{ij}^{(1)} = \frac{\pi(x_i)}{(x_i - x_j)\ \pi(x_j)} \qquad i,j = 1,2,\dots,N, \qquad i \neq j \tag{35}$$

in which $\pi(x_i)$ is defined by

$$\pi(x_i) = \prod_{j=1}^{N} (x_i - x_j), \qquad i \neq j \tag{36}$$

And when $i = j$

$$C_{ij}^{(1)} = c_{ii}^{(1)} = -\sum_{k=1}^{N} C_{ik}^{(1)}, \qquad i = 1,2,\dots,N, \qquad i \neq k, \qquad i = j \tag{37}$$

Then, weighting coefficients for high orders derivatives may be expressed by:

$$\begin{aligned}
C_{ij}^{(2)} &= \sum_{k=1}^{N} C_{ik}^{(1)} C_{kj}^{(1)} \\
C_{ij}^{(3)} &= \sum_{k=1}^{N} C_{ik}^{(1)} C_{kj}^{(2)} = \sum_{k=1}^{N} C_{ik}^{(2)} C_{kj}^{(1)} \\
C_{ij}^{(4)} &= \sum_{k=1}^{N} C_{ik}^{(1)} C_{kj}^{(3)} = \sum_{k=1}^{N} C_{ik}^{(3)} C_{kj}^{(1)} \qquad i,j = 1,2,\dots,N. \\
C_{ij}^{(5)} &= \sum_{k=1}^{N} C_{ik}^{(1)} C_{kj}^{(4)} = \sum_{k=1}^{N} C_{ik}^{(4)} C_{kj}^{(1)} \\
C_{ij}^{(6)} &= \sum_{k=1}^{N} C_{ik}^{(1)} C_{kj}^{(5)} = \sum_{k=1}^{N} C_{ik}^{(5)} C_{kj}^{(1)}
\end{aligned} \tag{38}$$

According to presented approach, the dispersions of grid points based upon Gauss-Chebyshev-Lobatto assumption are expressed as:

$$\begin{aligned}
x_i &= \frac{a}{2}\left[1 - \cos\left(\frac{i-1}{N-1}\pi\right)\right] \qquad i = 1,2,\dots,N, \\
y_j &= \frac{b}{2}\left[1 - \cos\left(\frac{j-1}{M-1}\pi\right)\right] \qquad j = 1,2,\dots,M,
\end{aligned} \tag{39}$$

Next, the time derivative for displacement components may be determined by

$$w_b(x,y,t) = W_b(x,y)e^{i\omega t} \tag{40}$$

$$w_s(x,y,t) = W_s(x,y)e^{i\omega t} \tag{41}$$

where W_b and W_n denote vibration amplitudes and ω defines the vibrational frequency. Then, it is possible to express obtained boundary conditions as:

$$\begin{aligned} & w_b = w_s = 0, \\ & \frac{\partial^2 w_b}{\partial x^2} = \frac{\partial^2 w_s}{\partial x^2} = \frac{\partial^2 w_b}{\partial y^2} = \frac{\partial^2 w_s}{\partial y^2} = 0 \\ & \frac{\partial^4 w_b}{\partial x^4} = \frac{\partial^4 w_s}{\partial x^4} = \frac{\partial^4 w_b}{\partial y^4} = \frac{\partial^4 w_s}{\partial y^4} = 0 \end{aligned} \tag{42}$$

Now, one can express the modified weighting coefficients for all edges simply-supported as:

$$\begin{aligned} & \bar{C}_{1,j}^{(2)} = \bar{C}_{N,j}^{(2)} = 0, \qquad i = 1,2,\ldots,M, \\ & \bar{C}_{i,1}^{(2)} = \bar{C}_{1,M}^{(2)} = 0, \qquad i = 1,2,\ldots,N. \end{aligned} \tag{43}$$

and

$$\bar{C}_{ij}^{(3)} = \textstyle\sum_{k=1}^{N} C_{ik}^{(1)} \bar{C}_{kj}^{(2)} \qquad \bar{C}_{ij}^{(4)} = \textstyle\sum_{k=1}^{N} C_{ik}^{(1)} \bar{C}_{kj}^{(3)} \tag{44}$$

By placing Eqs. (38)–(39) into Eqs. (30)–(33) and performing some simplifications leads to the following system based on mass matrix[M], stiffness matrix [K] and damping matrix [C] as:

$$\left\{ \{K] + i\bar{\omega}_n[C] + \bar{\omega}_n{}^2[M] \right\} \begin{Bmatrix} U_{mn} \\ V_{mn} \\ W_{bmn} \\ W_{smn} \end{Bmatrix} = 0 \tag{45}$$

Six grid points are adequate for convergence of the method. The presented results are based on the following dimensionless factors:

$$\hat{\omega} = \omega a\sqrt{\frac{\rho_c}{E_c}},\ K_w = \frac{k_w a^4}{D_c}, K_p = \frac{k_p a^2}{D_c}, C_d = c_d\frac{a^2}{\sqrt{\rho h D_c}}, \bar{N} = N\frac{a^2}{D_c}, D_c = \frac{E_c h^3}{12(1-v_c^2)} \tag{46}$$

5. Obtained results and discussions

The presented research examines vibration behaviors of hygro-thermally loaded porous FG nano-dimension plates based on four-variable plate model and DQ method. Nonlocal and strain gradient coefficients are used in order to define the size-dependent behavior of nano-size plate.

Table 1 Comparison of non-dimensional fundamental natural frequency $\hat{\omega} = \omega h \sqrt{\rho_c / G_c}$ of FG nanoplates with simply-supported boundary conditions (p=5)

a/h	μ	a/b=1		a/b=2	
		Natarajan *et al.* (2012)	present	Natarajan *et al.* (2012)	present
10	0	0.0441	0.043823	0.1055	0.104329
	1	0.0403	0.04007	0.0863	0.085493
	2	0.0374	0.037141	0.0748	0.074174
	4	0.0330	0.032806	0.0612	0.060673
20	0	0.0113	0.011256	0.0279	0.027756
	1	0.0103	0.010288	0.0229	0.022722
	2	0.0096	0.009534	0.0198	0.019704
	4	0.0085	0.008418	0.0162	0.016110

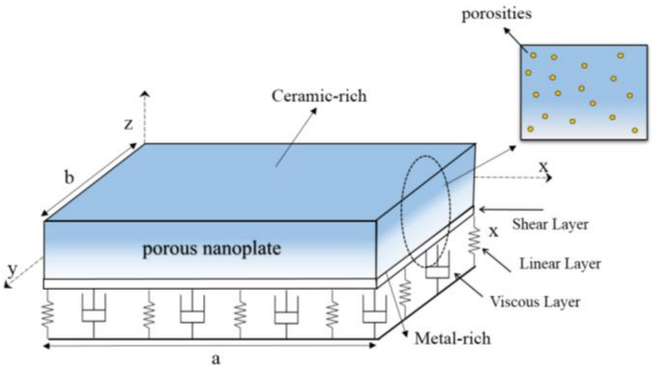

Fig. 1 Configuration of nanoporous inhomogeneous nanoplate on elastic substrate

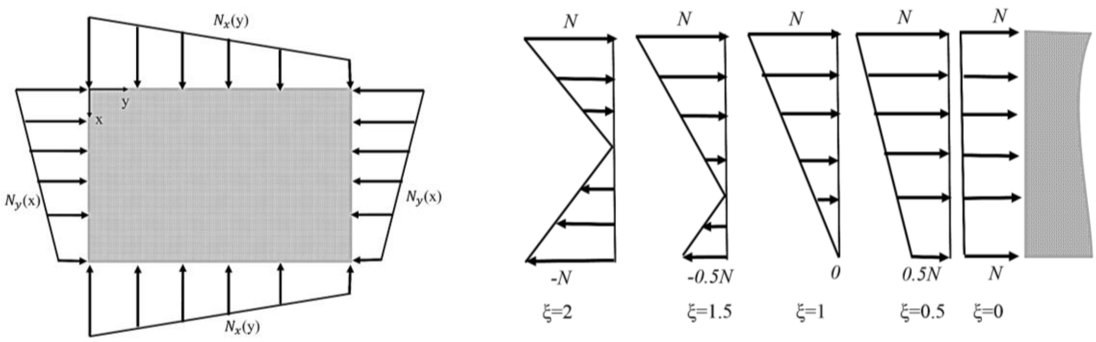

Fig. 2 Different cases of in-plane loads

Presented results indicate the prominence of moisture/temperature variation, damping factor, material gradient index, nonlocal coefficient, strain gradient coefficient and porosities on vibrational frequencies of FG nano-size plate. A verification study is presented in Table 1 for FG

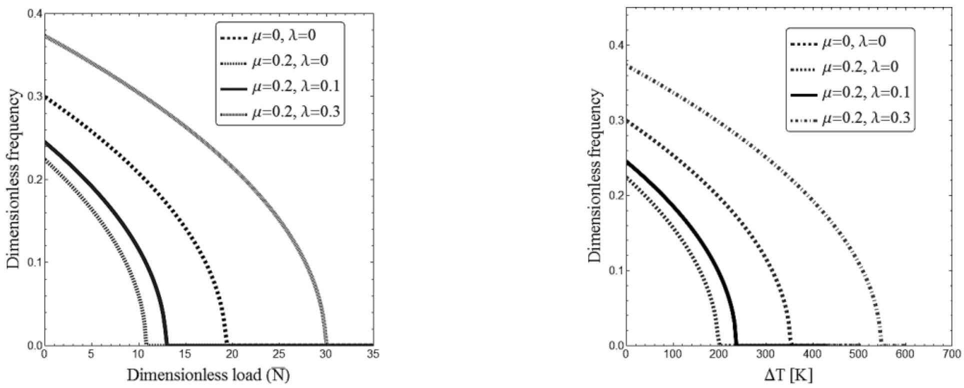

(a) Under mechanical load (b) Under thermal load

Fig. 3 Variation of dimensionless frequency of perfect nanoplate versus mechanical load and temperature rise for different nonlocal and strain gradient parameters (p=1, a/h=15, K_w=0, K_p=0, ΔC=0%)

nanoplate with comparing the vibrational frequency presented by DQM and those obtained by Natarajan *et al.* (2012). For presenting new results according to linearly varying in-plane loads, Fig. 2 shows all types of in-plane loadings. Also, each material property for FG plate may be assumed by:

$$E_c = 380\,GPa,\ \rho_c = 3800\ \ kg/m^3,\ v_c = 0.3,\ \gamma_c = 7\times10^{-6}\ \ 1/\ ^0C,\ \beta_c = 0.001\ \ (wt.\%\ \ H_2o)^{-1}$$

$$E_m = 70\,GPa,\ \rho_m = 2707\ \ kg/m^3,\ v_m = 0.3,\ \gamma_m = 23\times10^{-6}\ \ 1/\ ^0C,\ \beta_m = 0.44\ \ (wt.\%\ \ H_2o)^{-1}$$

In Fig. 3, the variation of normalized frequencies of a FG nano-dimension plate versus mechanical and thermal loading is represented for several nonlocality (μ) and stain gradients (λ) coefficients when *a/h*=15 and p=1. By selecting μ= λ=0, the vibrational frequencies based upon classic plate assumption will be derived. Actually, selecting λ=0 gives the frequency in the context of nonlocal elasticity theory (NET) and discarding strain gradients impacts. It can be understand from Fig. 3 that vibration frequency of system will rise with strain gradient coefficient and will reduce with nonlocality coefficient. This observation is valid for all kinds of applied loads. So, vibration behavior of the nanoplate system is dependent on both scale effects. Another finding is that increasing of temperature or in-plane mechanical load is corresponding to lower structural stiffness of the nano-dimension plate as well as smaller vibration frequency. At particular temperatures and in-plane mechanical loads, obtained frequency for the nanoplate will be zero. Therefore, when the frequency is zero, one can obtain critical buckling load and temperature. An important finding is that the critical buckling load and temperature are outstandingly affected by the values of nonlocal and strain gradient coefficients.

Fig. 4 indicates the impact of pore parameter on vibration frequency curves of porosity-dependent nano-sized plates when a=15h based on even pore dispersion. Different amounts of pore parameter have been selected (α=0, 0.1 and 0.2). The result based on α=0 is related to perfect nano-size plates. For both porous and perfect nano-size plate, the zero value of vibration frequency denotes the thermal buckling. One can find that the vibration frequencies become smaller by increasing in temperature value highlighting the intrinsic softening influence related to thermal loading. Then, one can find that increasing in pore parameter yields a lower vibration frequency at small values of temperature rise. The reason comes from the reduction of nano-sized plate stiffness

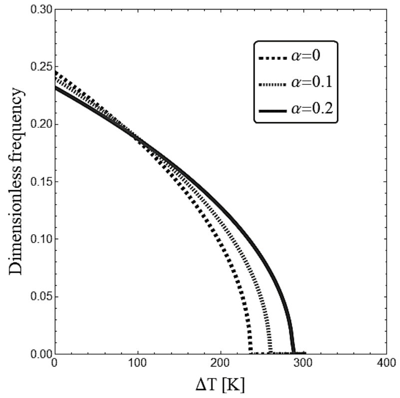

(a) p=1

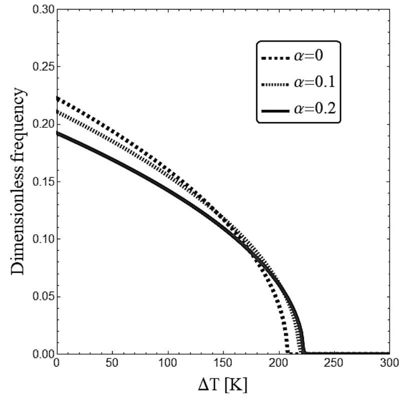

(b) p=2

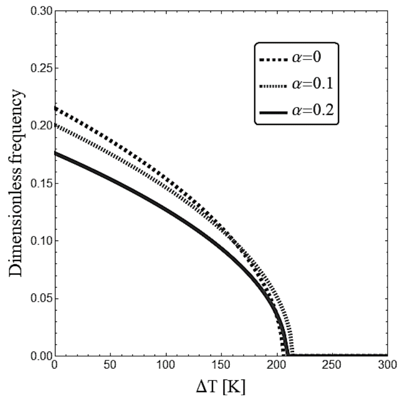

(c) p=3

Fig. 4 Variation of dimensionless frequency of porous nanoplates versus temperature change for different pore coefficients (a/h=15, ΔC=0%, K_w=0, K_p=0)

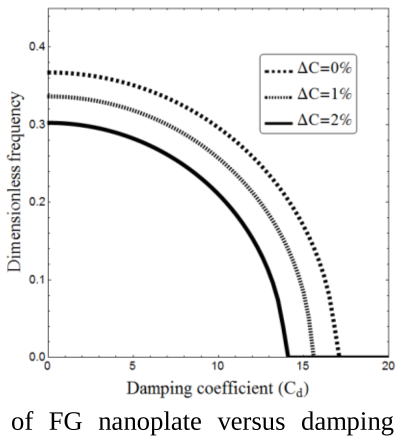

Fig. 5 Dimensionless frequency of FG nanoplate versus damping coefficient for various porosity coefficients (a/h=10, p=1, ΔT=10, K_w=5, K_p=0.5, μ=0.2, α=0.2, λ=0.1)

with the incorporation of porosities. However, at larger values of temperature rise, both porosity and thermal loading have notable influences on structural stiffness of the nanoplate.

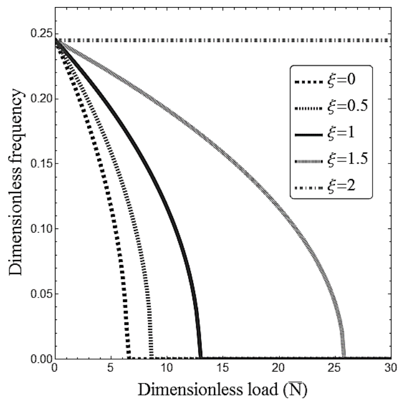

Fig. 6 Variation of dimensionless frequency versus dimensionless load for different load factors (a/h=15, p=1, ΔT=0, ΔC=0%, C_d=0, μ=0.2, λ=0.1)

Effects of moisture variation on damping vibrational behaviors of porous FG nanoplates at a/h=10, p=1, ΔT=10, K_w=5, K_p=0.5, μ=0.2 and λ=0.1 have been depicted in Fig. 5. It must be clarified that increasing in damping factor diminishes the structural stiffness and vibrational frequencies will decrease until a critical factor in which frequency magnitude becomes zero. The nano-dimension plate vibrations are damped at this point. It is also important to express that moisture rise yields lower normalized frequency. Actually, increasing in moisture value yields lower critical damping factors. Therefore, it may be deduced that hygro-thermal loads have great impacts on dynamic behavior of nano-dimension FG plates.

Fig. 6 illustrates the variation of normalized frequency for nano-dimension porous FG plate according to various types of applied mechanical loads at p=1, μ=0.2 and λ=0.1. In order to define the type of applied mechanical load, various values for load factor (ξ) have been determined. It is obvious that in-plane mechanical loads degrade the plate rigidity and affect notably the performance of a nano-size structure. One can see that increasing in load factor yields greater normalized frequency. Thus, critical buckling loads shift to the right. The reason is owing to reduced mechanical load resultant with increase of load factor.

6. Conclusions

The presented research examined vibration behaviors of hygro-thermally loaded porous FG nano-size plates based on four-variable plate model and DQ method. Nonlocal and strain gradient coefficients were used in order to define the size-dependent behavior of nano-size plate. It was seen that vibration frequency raised with strain gradient coefficient and reduced with nonlocality coefficient. Another finding was that increasing of temperature or in-plane mechanical load was corresponding to lower structural stiffness of the nano-dimension plate as well as smaller vibration frequency. Also, increase of porosity factor may reduce the value of vibrational frequency. It was stated that increasing in damping factor diminished the structural stiffness and vibrational frequencies decreased until a critical factor in which frequency magnitude became zero. It was found that increasing in moisture value led to lower critical damping factors.

References

Aissani, K., Bouiadjra, M.B., Ahouel, M. and Tounsi, A. (2015), "A new nonlocal hyperbolic shear deformation theory for nanobeams embedded in an elastic medium", *Struct. Eng. Mech.*, **55**(4), 743-763. https://doi.org/10.12989/sem.2015.55.4.743.

Alasadi, A.A., Ahmed, R.A. and Faleh, N.M. (2019), "Analyzing nonlinear vibrations of metal foam nanobeams with symmetric and non-symmetric porosities", *Adv. Aircraft Spacecraft Sci.*, **6**(4), 273-282. https://doi.org/10.12989/aas.2019.6.4.273.

Barati, M.R. and Zenkour, A. (2017), "A general bi-Helmholtz nonlocal strain-gradient elasticity for wave propagation in nanoporous graded double-nanobeam systems on elastic substrate", *Compos. Struct.*, **168**, 885-892. https://doi.org/10.1016/j.compstruct.2017.02.090.

Bekhadda, A., Cheikh, A., Bensaid, I., Hadjoui, A. and Daikh, A.A. (2019), "A novel first order refined shear-deformation beam theory for vibration and buckling analysis of continuously graded beams", *Adv. Aircraft Spacecraft Sci.*, **6**(3), 189-206. https://doi.org/10.12989/aas.2019.6.3.189.

Belkorissat, I., Houari, M.S.A., Tounsi, A., Bedia, E.A. and Mahmoud, S.R. (2015), "On vibration properties of functionally graded nano-plate using a new nonlocal refined four variable model", *Steel Compos. Struct.*, **18**(4), 1063-1081. http://doi.org/10.12989/scs.2015.18.4.1063.

Belmahi, S., Zidour, M. and Meradjah, M. (2019), "Small-scale effect on the forced vibration of a nano beam embedded an elastic medium using nonlocal elasticity theory", *Adv. Aircraft Spacecraft Sci.*, **6**(1), 1-18. https://doi.org/10.12989/aas.2019.6.1.001.

Bensaid, I. and Kerboua, B. (2019), "Improvement of thermal buckling response of FG-CNT reinforced composite beams with temperature-dependent material properties resting on elastic foundations", *Adv. Aircraft Spacecraft Sci.*, **6**(3), 207-223. https://doi.org/10.12989/aas.2019.6.3.207.

Berrabah, H.M., Tounsi, A., Semmah, A. and Adda, B. (2013), "Comparison of various refined nonlocal beam theories for bending, vibration and buckling analysis of nanobeams", *Struct. Eng. Mech.*, **48**(3), 351-365. https://doi.org/10.12989/sem.2013.48.3.351.

Besseghier, A., Heireche, H., Bousahla, A.A., Tounsi, A. and Benzair, A. (2015), "Nonlinear vibration properties of a zigzag single-walled carbon nanotube embedded in a polymer matrix", *Adv. Nano Res.*, **3**(1), 29-37. https://doi.org/10.12989/anr.2015.3.1.029.

Besseghier, A., Houari, M.S.A., Tounsi, A. and Mahmoud, S.R. (2017), "Free vibration analysis of embedded nanosize FG plates using a new nonlocal trigonometric shear deformation theory", *Smart Struct. Syst.*, **19**(6), 601-614. https://doi.org/10.12989/sss.2017.19.6.601.

Bouderba, B., Houari, M.S.A., Tounsi, A. and Mahmoud, S.R. (2016), "Thermal stability of functionally graded sandwich plates using a simple shear deformation theory", *Struct. Eng. Mech.*, **58**(3), 397-422. https://doi.org/10.12989/sem.2016.58.3.397.

Bouadi, A., Bousahla, A.A., Houari, M.S.A., Heireche, H. and Tounsi, A. (2018), "A new nonlocal HSDT for analysis of stability of single layer graphene sheet", *Adv. Nano Res.*, **6**(2), 147-162. https://doi.org/10.12989/anr.2018.6.2.147.

Chikh, A., Bakora, A., Heireche, H., Houari, M.S.A., Tounsi, A. and Bedia, E.A. (2016), "Thermo-mechanical postbuckling of symmetric S-FGM plates resting on Pasternak elastic foundations using hyperbolic shear deformation theory", *Struct. Eng. Mech.*, **57**(4), 617-639. https://doi.org/10.12989/sem.2016.57.4.617.

Daneshmehr, A. and Rajabpoor, A. (2014), "Stability of size dependent functionally graded nanoplate based on nonlocal elasticity and higher order plate theories and different boundary conditions", *Int. J. Eng. Sci.*, **82**, 84-100. https://doi.org/10.1016/j.ijengsci.2014.04.017.

Ebrahimi, F. and Barati, M.R. (2016a), "Size-dependent thermal stability analysis of graded piezomagnetic nanoplates on elastic medium subjected to various thermal environments", *Appl. Phys. A*, **122**(10), 910. https://doi.org/10.1007/s00339-016-0441-9.

Ebrahimi, F. and Barati, M.R. (2017), "Hygrothermal effects on vibration characteristics of viscoelastic FG nanobeams based on nonlocal strain gradient theory", *Compos. Struct.*, **159**, 433-444.

https://doi.org/10.1016/j.compstruct.2016.09.092.

Ebrahimi, F., Barati, M.R. and Dabbagh, A. (2016), “A nonlocal strain gradient theory for wave propagation analysis in temperature-dependent inhomogeneous nanoplates”, *Int. J. Eng. Sci.*, **107**, 169-182. https://doi.org/10.1016/j.ijengsci.2016.07.008.

El-Hassar, S. M., Benyoucef, S., Heireche, H. and Tounsi, A. (2016), “Thermal stability analysis of solar functionally graded plates on elastic foundation using an efficient hyperbolic shear deformation theory”, *Geomech. Eng.*, **10**(3), 357-386. https://doi.org/10.12989/gae.2016.10.3.357.

Elmerabet, A. H., Heireche, H., Tounsi, A. and Semmah, A. (2017), “Buckling temperature of a single-walled boron nitride nanotubes using a novel nonlocal beam model”, *Adv. Nano Res.*, **5**(1), 1-12. https://doi.org/10.12989/anr.2017.5.1.001.

Eringen, A.C. (1983), “On differential equations of nonlocal elasticity and solutions of screw dislocation and surface waves”, *J. Appl. Phys.*, **54**(9), 4703-4710. https://doi.org/10.1063/1.332803.

Fenjan, R.M., Ahmed, R.A., Alasadi, A.A. and Faleh, N.M. (2019), “Nonlocal strain gradient thermal vibration analysis of double-coupled metal foam plate system with uniform and non-uniform porosities”, *Coupled Syst. Mech.*, **8**(3), 247-257. https://doi.org/10.12989/csm.2019.8.3.247.

Jabbari, M., Vaghari, A.R., Bahtui, A. and Eslami, M.R. (2008), “Exact solution for asymmetric transient thermal and mechanical stresses in FGM hollow cylinders with heat source”, *Struct. Eng. Mech.*, **29**(5), 551-565. https://doi.org/10.12989/sem.2008.29.5.551.

Lal, A., Jagtap, K.R and Singh, B.N. (2017), “Thermo-mechanically induced finite element based nonlinear static response of elastically supported functionally graded plate with random system properties”, *Adv. Comput. Des.*, **2**(3), 165-194. https://doi.org/10.12989/acd.2017.2.3.165.

Lam, D.C., Yang, F., Chong, A.C.M., Wang, J. and Tong, P. (2003), “Experiments and theory in strain gradient elasticity”, *J. Mech. Phys. Solids*, **51**(8), 1477-1508. https://doi.org/10.1016/S0022-5096(03)00053-X.

Larbi Chaht, F., Kaci, A., Houari, M.S.A., Tounsi, A., Anwar Bég, O. and Mahmoud, S.R. (2015), “Bending and buckling analyses of functionally graded material (FGM) size-dependent nanoscale beams including the thickness stretching effect”, *Steel Compos. Struct.*, **18**(2), 425-442. https://doi.org/10.12989/scs.2015.18.2.425.

Lee, Z., Ophus, C., Fischer, L.M., Nelson-Fitzpatrick, N., Westra, K.L., Evoy, S. and Mitlin, D. (2006), “Metallic NEMS components fabricated from nanocomposite Al–Mo films”, *Nanotechnology*, **17**(12), 3063. https://doi.org/10.1088/0957-4484/17/12/042.

Li, L., Hu, Y. and Ling, L. (2015), “Flexural wave propagation in small-scaled functionally graded beams via a nonlocal strain gradient theory”, *Compos. Struct.*, **133**, 1079-1092. https://doi.org/10.1016/j.compstruct.2015.08.014.

Li, L., Li, X. and Hu, Y. (2016), “Free vibration analysis of nonlocal strain gradient beams made of functionally graded material”, *Int. J. Eng. Sci.*, **102**, 77-92. https://doi.org/10.1016/j.ijengsci.2016.07.011.

Li, L. and Hu, Y. (2015), “Buckling analysis of size-dependent nonlinear beams based on a nonlocal strain gradient theory”, *Int. J. Eng. Sci.*, **97**, 84-94. https://doi.org/10.1016/j.ijengsci.2015.08.013.

Li, L. and Hu, Y. (2016), “Nonlinear bending and free vibration analyses of nonlocal strain gradient beams made of functionally graded material”, *Int. J. Eng. Sci.*, **107**, 77-97.

Li, L. and Hu, Y. (2017), “Post-buckling analysis of functionally graded nanobeams incorporating nonlocal stress and microstructure-dependent strain gradient effects”, *Int. J. Mech. Sci.*, **120**, 159-170. https://doi.org/10.1016/j.ijmecsci.2016.11.025.

Lim, C. W., Zhang, G. and Reddy, J.N. (2015), “A higher-order nonlocal elasticity and strain gradient theory and its applications in wave propagation”, *J. Mech. Phys. Solids*, **78**, 298-313. https://doi.org/10.1016/j.jmps.2015.02.001.

Mirsalehi, M., Azhari, M. and Amoushahi, H. (2017), “Buckling and free vibration of the FGM thin micro-plate based on the modified strain gradient theory and the spline finite strip method”, *Eur. J. Mech. A/Solids*, **61**, 1-13. https://doi.org/10.1016/j.euromechsol.2016.08.008.

Natarajan, S., Chakraborty, S., Thangavel, M., Bordas, S. and Rabczuk, T. (2012), “Size-dependent free flexural vibration behavior of functionally graded nanoplates”, *Comput. Mater. Sci.*, **65**, 74-80.

https://doi.org/10.1016/j.commatsci.2012.06.031.
Sedighi, H.M., Daneshmand, F and Abadyan, M. (2015), "Modified model for instability analysis of symmetric FGM double-sided nano-bridge: corrections due to surface layer, finite conductivity and size effect", *Compos. Struct.*, **132**, 545-557. https://doi.org/10.1016/j.compstruct.2015.05.076.
Sobhy, M. (2015), "A comprehensive study on FGM nanoplates embedded in an elastic medium", *Compos. Struct.*, **134**, 966-980. https://doi.org/10.1016/j.compstruct.2015.08.102.
Sobhy, M. (2016), "An accurate shear deformation theory for vibration and buckling of FGM sandwich plates in hygrothermal environment", *Int. J. Mech. Sci.*, **110**, 62-77. https://doi.org/10.1016/j.ijmecsci.2016.03.003.
Sobhy, M. and Radwan, A.F. (2017), "A new quasi 3D nonlocal plate theory for vibration and buckling of FGM nanoplates", *Int. J. Appl. Mech.*, 1750008. https://doi.org/10.1142/S1758825117500089.
Tang, H., Li, L., Hu, Y., Meng, W. and Duan, K. (2019), "Vibration of nonlocal strain gradient beams incorporating Poisson's ratio and thickness effects", *Thin-Walled Struct.*, **137**, 377-391. https://doi.org/10.1016/j.tws.2019.01.027.
Yazid, M., Heireche, H., Tounsi, A., Bousahla, A.A. and Houari, M.S.A. (2018), "A novel nonlocal refined plate theory for stability response of orthotropic single-layer graphene sheet resting on elastic medium", *Smart Struct. Syst.*, **21**(1), 15-25. https://doi.org/10.12989/sss.2018.21.1.015.
Zalesak, J., Bartosik, M., Daniel, R., Mitterer, C., Krywka, C., Kiener, D and Keckes, J. (2016), "Cross-sectional structure-property relationship in a graded nanocrystalline Ti 1− x Al x N thin film", *Acta Materialia*, **102**, 212-219. https://doi.org/10.1016/j.actamat.2015.09.007.
Zenkour, A.M. and Abouelregal, A.E. (2014), "The effect of two temperatures on a FG nanobeam induced by a sinusoidal pulse heating", *Struct. Eng. Mech.*, **51**(2), 199-214. https://doi.org/10.12989/sem.2014.51.2.199.
Zenkour, A.M. and Abouelregal, A.E. (2014), "Decaying temperature and dynamic response of a thermoelastic nanobeam to a moving load", *Coupled Syst. Mech.*, **3**(1), 1-16. https://doi.org/10.12989/acd.2018.3.1.001.

GY